Compensation of Shallow Donors by Gallium Vacancies in Monoclinic β-math xmlns="http://www.w3.org/1998/Math/MathML" display="inline" overflow="scroll">msub>mi>Ga /mi>mn>2/mn>/msub>msub>mrow>mrow>mi mathvariant="normal">O/mi>/mrow>/mrow>mn>3/mn>/ msub>/math>

Santosh K. Swain, Marc H. Weber, Jani Jesenovec, Muad Saleh, Kelvin G. Lynn, and John S. McCloy

Phys. Rev. Applied **15**, 054010 — Published 5 May 2021

DOI: 10.1103/PhysRevApplied.15.054010

Compensation of shallow donors by gallium vacancies in monoclinic β-Ga_2O_3

Santosh K. Swain, Marc H. Weber, Jani Jesenovec, Muad Saleh, Kelvin G. Lynn,[†] John S. McCloy[*]

Institute for Materials Research, Washington State University, Pullman, WA 99164, USA.

Abstract

Knowledge of the origin of deep levels and their impact on electrical properties is critical for device applications of β-Ga_2O_3. By annealing under oxygen (O_2) atmosphere, the resistivity in shallow donor (zirconium) doped β-Ga_2O_3:Zr single crystals is found to increase by more than ten orders of magnitude to $(7\pm4)\times10^{10}$ Ω·cm, comparable to the resistivity achieved by iron (Fe) acceptor doping $(5\pm3)\times10^{11}$ Ω·cm. We combine thermo-electric effect spectroscopy (TEES) and positron annihilation spectroscopy (PAS), which are sensitive to deep levels and concentration of open volume defects, with modelling of the electrical properties, to study these strongly compensated crystals. We find the compensating level in the O_2 annealed β-Ga_2O_3:Zr sample to be located at 0.727±0.021 eV (E2*) below the conduction band which correlates with a vacancy signal from PAS data. The defect is most likely the relaxed split Ga vacancy V^i_{Ga} rather than a simple gallium vacancy considering theoretical predictions of a small energy barrier to relax. We observe that, due to the unique nature of these vacancies and anisotropy in the monoclinic lattice, the Doppler broadening parameter is rather small compared to other wide gap compounds, and in such a case positron diffusion length is a suitable parameter to estimate open volume defect concentration.

I. INTRODUCTION

[†]deceased
[*]corresponding author, john.mccloy@wsu.edu

Ultra-wide band gap (UWBG) β-Ga_2O_3 is emerging as the material of choice for next generation power electronics suitable for high voltage and high frequency operations, UV detectors, high temperature gas sensors, and potential nano-photonic devices, due to its attractive properties including large band gap ≈4.8 eV, high breakdown field of ≈8 MV/cm, low on-state resistance, and availability of low defect density native substrates both highly n-type and semi-insulating [1–8]. Similar to many other wide gap oxides, high p-type conductivity is challenging to obtain, due to the localized oxygen p-orbital, and hole self-trapping [9]. High n-type conductivity is typically obtained by doping with Si, Sn, or Ge [10]. Recently, we demonstrated similar or higher electron concentration with zirconium (Zr) or hafnium (Hf) doping, with additional advantages of higher mobility, higher dopant solubility, and lower dopant vapor pressure [11,12].

Acceptors in β-Ga_2O_3 are deep, and these defects can influence the electrical and optical properties as compensation and recombination centers. Deep extrinsic acceptors Fe and Mg are known to cause high resistivity and are used to obtain semi-insulating wafers by various melt growth techniques. In the present investigation we report that high resistivity, comparable to that obtained by deep acceptor doping, is achieved by annealing shallow donor-doped crystals under oxygen (O_2) atmosphere and creating a sufficient concentration of native defects. Among the possible native defects, the formation of gallium vacancies (V_{Ga}) and associated defect complexes with hydrogen are thermodynamically favorable under oxygen-rich conditions for Fermi level positions closer to the conduction band, and they are predicted to be deep acceptors [13–15]. Techniques such as electron paramagnetic resonance and infrared spectroscopy studies have identified these defects [16–18]. Positron annihilation studies have shown high concentration of open volume defects related to V_{Ga} under oxygen-rich conditions

which caused compensation of Si donors [19,20]. Deep acceptors with various energy levels have been reported to reduce the n-type conductivity in donor-doped and undoped β-Ga_2O_3 films and bulk crystals [21–24].

The techniques that are commonly employed to determine the energy levels and defect concentrations, based on capacitance transients, generally use conductive samples with free electron concentrations ~10^{16} cm^{-3} or higher, but these measurements are challenging when the material becomes semi-insulating. Further, the presence of an electric field during emission from the traps is reported to alter the estimated trap parameters due to field enhanced emission rates [25]. In order to quantitatively describe electrical compensation in shallow donor-doped β-Ga_2O_3 and identify the origin of the involved defect, we apply thermo electric effect spectroscopy (TEES) that is sensitive to deep levels in semi-insulating materials and positron annihilation spectroscopy (PAS) with its sensitivity to vacancy type defects in neutral and negative charge state [26,27].

II. EXPERIMENTAL METHODS

A. Thermo-Electric Effect Spectroscopy

In this study, two types of bulk single crystals are investigated by TEES. One is a zirconium-doped crystal (β-Ga_2O_3:Zr), with room temperature electron concentration ≈5×10^{17} cm^{-3}, that was cleaved in (100) orientation from a Czochralski (CZ) grown boule. The growth and electrical properties are described elsewhere [11]. The crystal was annealed at 1050 °C or 1400 °C for 15 hours in an oxygen atmosphere. The second sample is a CZ grown Fe-doped crystal provided by Northrup Grumman Synoptics. The orientation for the Fe-doped sample is not measured but believed to be either (100) or (001), as it was easy to cleave layers from the sample surface. TEES measurement involves trap filling at a low temperature by optical

excitation followed by thermal emission from the trap during heat up. In TEES, the driving force to extract thermally emitted carriers is a temperature gradient rather than a bias across the thickness of the sample. The technique works best for materials with low thermal conductivity and is particularly suitable for high resistivity materials where the dark current is low enough to allow observation of current signal from traps, which is typically of the order of few pico amps (pA). TEES has been applied in the past to semi-insulating GaAs [28], GaN [29], CdZnTe [30], and CdTe [31], to identify native defects, dopants, and complexes. The energy level of the traps can be extracted from the initial onset of the current or by applying different heating rates in multiple scans, i.e., the variable heating rate method (VHR). The VHR method commonly used in conductivity glow curve analysis [32] is used to estimate the trap energies and cross section using equation 1.

$$\ln\left(\frac{T_M^2}{\beta}\right) = \frac{E_{th}}{k_B T_M} - \ln\left(\frac{\sigma_{th} \nu_n N_c k_B}{E_{th}}\right) \quad (1)$$

E_{th} is thermal ionization energy, T_M is temperature corresponding to maximum current, β is heating rate with units K/s, k_B is Boltzmann's constant, σ_{th} is trapping cross section, ν_n is carrier thermal velocity, and N_c is effective density of states.

Samples for TEES measurements had area ≈8×8 mm^2 and (1-2) mm thickness. Planar contacts of Ga+In were applied on the top and bottom surfaces of the sample and connected to a Keithley 6517 electrometer for current measurement. The samples were illuminated with sub-bandgap photons (365 nm, 385 nm, or 400 nm), for 1000 s at a low temperature. TEES spectra were collected by heating up the sample at constant rates between 0.05 K/s to 0.3 K/s, with an imposed temperature gradient of 10 K across the thickness.

B. Positron Annihilation Spectroscopy

Samples for PAS included, in addition to the two samples studied by TEES, an undoped crystal grown using high purity Ga_2O_3 powder labelled as HP, an unintentionally doped (UID) sample in the as-grown not annealed state (UID-na) and following annealing in O_2 at 1050 °C or 1400 °C, and a Zr-doped sample annealed at 1400 °C. We employed Doppler broadened PAS, with a monoenergetic variable energy positron beam up to 70 keV, equivalent to a mean implantation depth of ~6.3 μm in β-Ga_2O_3. After implantation in the sample, the positron thermalizes in a few picoseconds followed by thermal diffusion and possible trapping at open volume defects, if present in neutral or negative charge state, leading to an increase in annihilations with low momentum delocalized electrons. Doppler broadening is measured with a pair of high purity Germanium (HPGe) detectors with an energy resolution of 1.45 keV full-width half maximum (FWHM) at 511 keV and high detection efficiency of >100% relative to NaI scintillators. The second detector is used in coincidence to veto against positrons that backscatter from the sample and annihilate near but not on the sample, a systematic effect that cannot be ignored for materials with high average atomic number (Z) and high density such as Ga_2O_3.

The Doppler broadening signal is composed of annihilation events in a narrow central 1.5 keV wide window of the 511 keV annihilation peak, the *S*-parameter, and a partially anti-correlated signal from the wings of the peak, the *W*-parameter 2.6 to 5.85 keV from the peak. *S* and *W* are normalized by the total peak rate in a 11.7 keV window after background subtraction. When positrons trap in vacancies prior to annihilation the central *S* fraction increases, and the *W* fraction decreases with increasing concentration in vacancies. In contrast, the peak is broadened for annihilations in a defect-free lattice where the positron annihilates from its delocalized bulk state carrying contributions from high momentum core electrons. *W* also contains annihilations

with high momentum electrons bound to atoms next to the vacancy. This adds a defect-type specific component to *W*. A linear correlation of *S* vs. *W* with a constant slope indicates changes in the concentration of a single defect type. Changes in slope point to changes in the defect type. The dynamic range is determined by the bulk *S* value (S_b) for defect-free lattice and the *S* value for saturation trapping (S_d) when all the positrons annihilate from a trapped state. The dynamic range typically spans about 6 orders of magnitude in defect concentration. However, the technique is most sensitive to defect concentration (c_d) in the $\approx 1\times10^{16}$ cm^{-3} to $\approx 5\times10^{18}$ cm^{-3} range. The vacancy defect concentration c_d is estimated using equation 2.

$$c_d = \frac{N}{\mu \cdot \tau} \cdot \frac{S - S_b}{S_d - S} \tag{2}$$

N: number density of atoms 1.88×10^{22} cm^{-3} for Ga_2O_3; μ: specific trapping rate $\sim 3\times10^{15}$/s [27] [33] for negatively charged vacancies; and τ: positron lifetime in the defect-free lattice for which a value of 176 ps is used [19]. Like in many other novel crystalline materials, particularly when they are more complex than basic semiconductors as silicon and germanium, a perfect defect-free reference sample is not available. The estimation of a defect concentration remains that, an estimate. A crystal grown at WSU from high purity starting material, however, shows evidence of high quality from a positron perspective. A bulk lifetime measurement is consistent with a single lifetime of 176 ps. A longer component on the order of 400 ps with an intensity of several percent is likely due to the ^{22}Na source deposited directly onto the sample. 176 ps is consistent with the lifetime reported by W.Y. Ting et al. [Materials Science and Engineering B91–92 541–544 (2002)]. Vepfit of depth profile data in the [001] orientation yields a good fit with a single layer and $S_{layer} = 0.4160\pm0.0003$ and a diffusion length of $L = 92\pm8$ nm.

Unlike more commonly studied semiconductors, the electronic structure of β-Ga_2O_3 is highly anisotropic [34]. The Doppler signature is found to change depending on the direction of the emitted annihilation photons relative to the lattice orientation. Secondly, the gallium vacancy (V_{Ga}), which can exist on a tetrahedral as well as on an octahedral site, is also found to relax into a split configuration where a gallium atom sits on an interstitial site between two gallium vacancies V^{i}_{Ga} of which 3 configurations are possible, due to the low energy barrier of ~0.53 eV to relax into the split state is 0.53 eV [35]. Karjalainen et. al. [34] has shown that this leads to an unusually small vacancy Doppler signal *S* of only about 2 to 3% above defect-free Ga_2O_3. The values are used in lieu of a perfect sample. The Doppler value of S = 0.4160 for the [001] orientation is the lowest and the result for the [010] orientation is about 2% higher, consistent with the work reported in ref. [34].

The defect concentration c_d can also be estimated from the measured positron diffusion length *L*, which is another defect-sensitive parameter in PAS. In defect-free material, it reflects the finite lifetime of positrons. Depth profiles of positron annihilations can be used to extract the positron diffusion length. The observed depth profile is a convolution of the actual damage depth profile with the implantation profile and the diffusion of thermal positrons until trapping or annihilation from the defect-free state. The diffusion length decreases L_b (bulk value) to L_d (saturation trapping) with increasing concentration of trapping defects c_d, which can be estimated using equation 3.

$$c_d = \frac{N}{\mu.\tau}\left(\frac{L_b^2}{L_d^2} - 1\right) \tag{3}$$

The values obtained from the high-purity source material sample are used to estimate the defect concentration: S_b = 0.4160 and (S_d ~1.03·S_b), and a diffusion length of L_b = 100 nm ≥ 92nm in

the same sample. The resulting defect concentrations should be considered as lower limits based on the uncertainty about the "defect-free" nature of the reference sample.

Theoretical work on β-Ga_2O_3 predicts a positron wave function aligned as near 1D channels along the [001] axis along tubes of the larges open space in the crystal lattice and perpendicular to the main cleavage plane. Implanting positrons in this direction and detecting the Doppler signal in the two perpendicular directions yields the lowest and highest S as a function of orientation. The diffusion of positrons however, is independent of this quasi rotation of the detector around the sample. Diffusion or tunneling of positrons perpendicular to this direction is possible. The diffusion length $_L$ has a larger dynamic range than the relatively small range in S of 2 to 3%. L may be a better measure of the defect concentration in Ga_2O_3.

III. RESULTS AND DISCUSSION

A. Electrically Compensating Acceptor Levels Observed in TEES

Following oxygen annealing, the resistivity of the β-Ga_2O_3:Zr sample increased by nearly 10 orders of magnitude from ≈0.1 Ω·cm to ≈7×10^{10} Ω·cm, whereas the as-grown Fe-doped sample had resistivity (5±3) $\times10^{11}$ Ω·cm. The current versus voltage (I-V) characteristics of these samples are shown in Fig. 1.

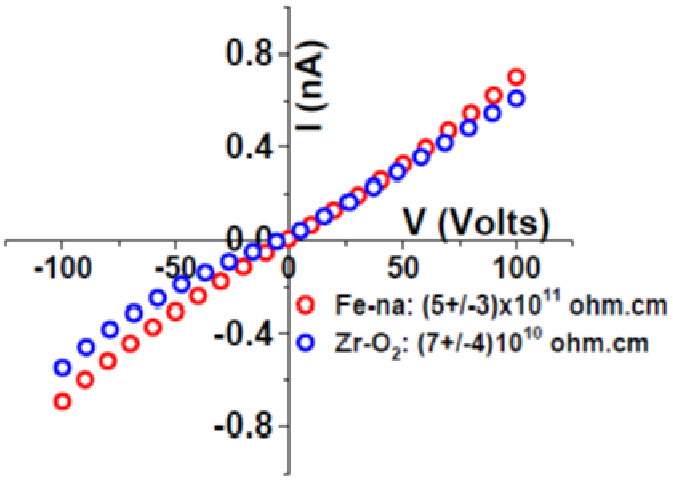

FIG. 1, I-V characteristics of O_2 annealed Zr-doped sample, and Fe-doped not annealed (Fe-na) crystal.

High resistivity in Fe-doped crystals is known to be caused by Fe acceptors located (0.75-0.82) eV below the conduction band [36] [37]. Here we investigated the origin of high resistivity in the O_2 annealed β-Ga_2O_3:Zr. Two prominent defect levels (TEES current peaks) at ≈175 K and ≈280 K are observed in the TEES spectrum for this sample as shown in Fig. 2.

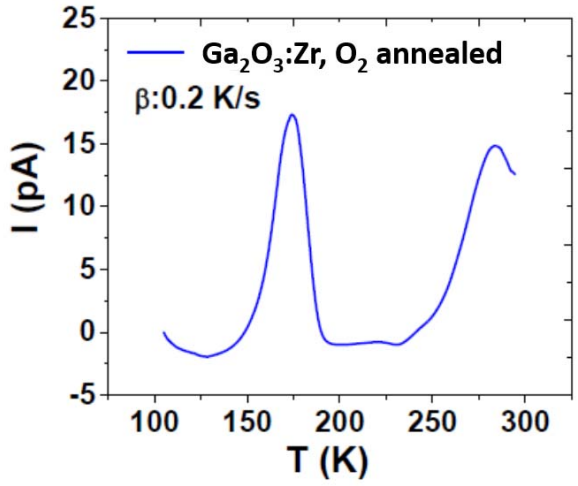

FIG. 2, TEES spectrum of O_2 annealed β-Ga_2O_3:Zr sample, obtained with a heating rate of 0.2 K/s, and illumination with 365 nm at 100 K.

Arrhenius fits using equation 1 estimated energies of 0.573 ± 0.030 eV and 0.727 ± 0.021 eV, respectively, for the traps observed near 175 K and 280 K. Deep electron traps with similar energies have been reported in various β-Ga_2O_3 single crystals and films; however, their origins are not clearly determined [24] [38] [39].

The VHR method used here to estimate the trap energy assumes negligible re-trapping of the emitted carriers. In cases when recombination is not monomolecular, the VHR method can give erroneous values for trap parameters. We also applied the initial rise method, which disregards any recombination kinetics, since very early in the trap emptying process, far from the temperature corresponding to maximum TEES current (T_M), the emission is thermally activated. However, the technique is sensitive to the selection of initial current. Therefore, to avoid distortions in the current baseline, the trap filling was performed at a temperature (180 K) where the lower temperature traps are left empty. Fig. 3(a) and (b) show the energy of the trap near 280 K determined by VHR method (0.727 +/- 0.021 eV) and initial rise method (0.734±0.008 eV), confirming the accuracy of the estimated energy.

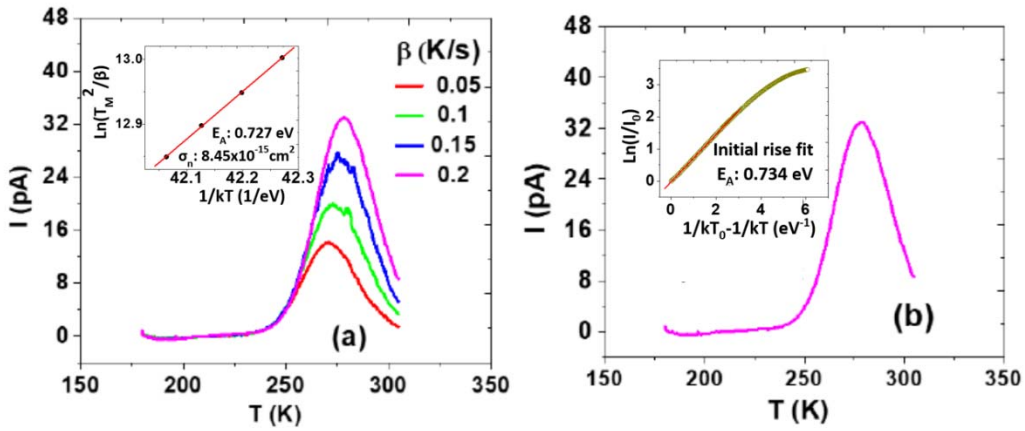

FIG. 3, (a) VHR TEES spectra and Arrhenius fit for the 280 K peak of the O_2 annealed β-Ga_2O_3:Zr with energy 0.727 eV, and (b) energy estimated by initial rise method ≈0.734 eV.

Here, in order to quantitatively describe the compensation in the O_2 annealed β-Ga_2O_3:Zr, sample, we model the resistivity, taking into account the observed traps at 0.573 eV and 0.73 eV and the measured values for donor concentration N_D (5×10^{17} cm^{-3}) and energy level E_D (15 meV) before annealing [11]. Using charge neutrality equation 4 we obtain the resistivity as a function of concentration of deep acceptors (N_A) with energies (E_A) at ≈0.573 eV and ≈0.73 eV below the conduction band.

$$p + \frac{N_D}{1+g_D \cdot e^{\frac{E_f - E_D}{kT}}} = n + \frac{N_A}{1+g_A \cdot e^{\frac{E_A - E_f}{kT}}} \quad (4)$$

Here p and n are free hole and electron concentrations, respectively. The degeneracy factors for donor and acceptor levels are g_D and g_A, respectively, and E_f is the position of the Fermi level (E_f) with reference to the valence band edge.

Fig. 4 shows the E_f positions and the resistivity as the acceptor concentrations are varied in the 10^{16} cm^{-3} to 10^{19} cm^{-3} range. Clearly, the measured resistivity of ≈7×10^{10} Ω·cm is attained with the 0.73 eV trap, at concentrations ≈1×10^{18} cm^{-3} or higher, whereas the 0.57 eV trap is too shallow to pull the Fermi level deep enough to cause the observed resistivity. The origin of the level at 0.573 eV could not be identified from this study; however, levels with energy (0.5-0.6) eV have been reported to be likely associated with metallic impurities [24] [39].

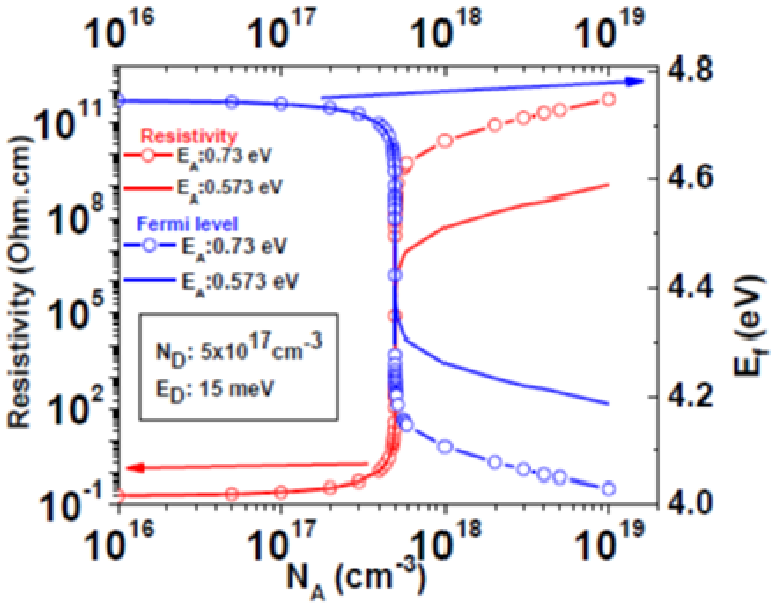

FIG. 4, Modeled Fermi level position and resistivity in the O_2 annealed β-Ga_2O_3:Zr sample as a function of concentration of acceptors at 0.57 eV and 0.73 eV below conduction band.

We next compared these defects in the annealed donor-doped sample with those measured on the unannealed acceptor-doped (Fe-na) sample. As shown in Fig. 5(a), two levels near ≈275 K and ≈320 K are prominent. The energy of the level near 275 K is estimated to be ≈0.73 eV by VHR method, indicating that the level is common to the Fe-doped and annealed Zr-doped samples. The dominant level near 320 K has energy 0.810±0.028 eV as shown in Fig. 5(b). Several studies report a level in the energy range, 0.7-0.8 eV. Our results indicate that there are in fact two closely spaced defects in this range. This is in agreement with Ingebrigtsen et al. [37], , who report levels at 0.75 eV and 0.78 eV, with the former assigned to a native defect because of its appearance upon proton irradiation, and the latter to a Fe acceptor. We assign the 0.81 eV level to Fe acceptors responsible for the high resistivity in the as grown Fe doped sample. On the other hand, the common ~ 0.73 eV level in the O_2 annealed β-Ga_2O_3:Zr, sample and Fe-doped as grown sample is likely associated with a native defect, which we further show below to be related to V_{Ga}.

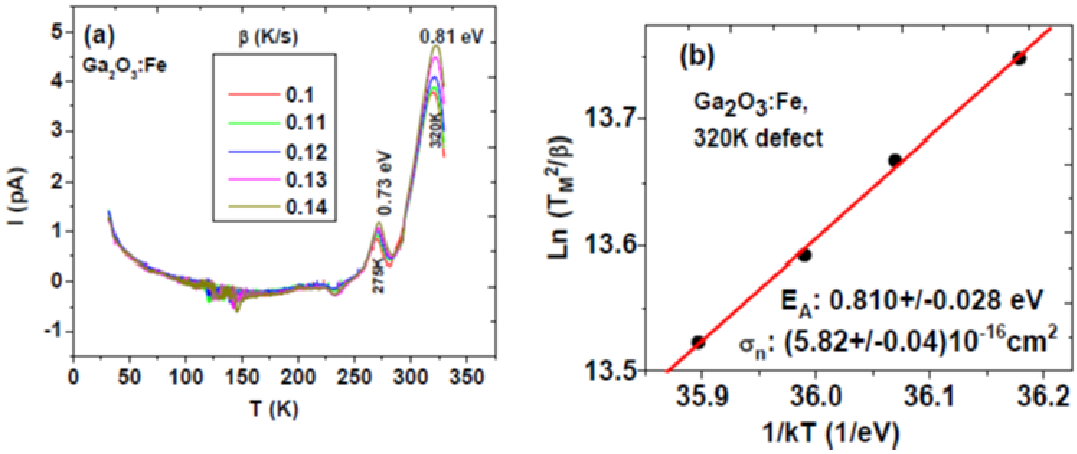

FIG. 5, (a) VHR TEES spectra for Fe doped sample and (b) Arrhenius fit using equation 1 the peak near 320 K.

B. Confirmation of the Native Defect Identity by PAS

The type and concentration of open volume defects is determined from PAS data. As noted earlier, Ga_2O_3 poses several challenges to PAS measurements. Determination of defect concentration, using equation 2, requires S_b value for each of the crystallographic orientations. However, reliable determination of S_b for all orientations is missing due to the lack of measurements on high-quality defect-free Ga_2O_3 samples. Among the various samples characterized in our laboratory using PAS, the lowest S value is measured on an UID crystal grown by CZ method using high purity Ga_2O_3 source powder, referred to as HP. This lowest value of S=0.4160±0.0003 is measured along the [001] direction and is used as S_b for estimating c_d. The PAS data are presented in Fig. 6. The data presented in Fig 6 (a) display one type of annihilation at the surface (high S) and a single layer throughout the depth probed by the positron beam (~6.3 μm). A custom fitting program VEPFit[41] is applied to deconvolute the positron implantation profile from the diffusion length and provides S values for distinct layers of a damage depth profile [40]. Simple layers with constant annihilation characteristics are used. Fits are shown as solid lines in the figure. The bulk S - W data are shown in Fig 6(b). For clarity in

the figure, only the HP sample and the Zr-doped sample annealed under O_2 at 1050 °C are shown in Fig 6 (a), whereas in the *S*-*W* plot of Fig 6 (b), we have also included the as-grown Fe-doped sample, an UID sample in the as-grown not annealed state (UID-na) and following annealing in O_2 at 1050 °C or 1400 °C, and a Zr-doped sample annealed at 1400 °C. The resistivity in the UID samples were also observed to increase by various orders of magnitude depending on annealing conditions.

Using the reported small dynamic range of <3% (S_d ~1.03·S_b) for Ga-vacancy defects in Ga_2O_3, and the measured bulk *S* value of the samples, which are found to be in the range from 2.25% above S_b up to the upper end of the dynamic range, with respect to the HP sample, c_d is estimated to be in the range from ≈ 1×10^{17} cm^{-3} to 5×10^{18} cm^{-3} or higher.

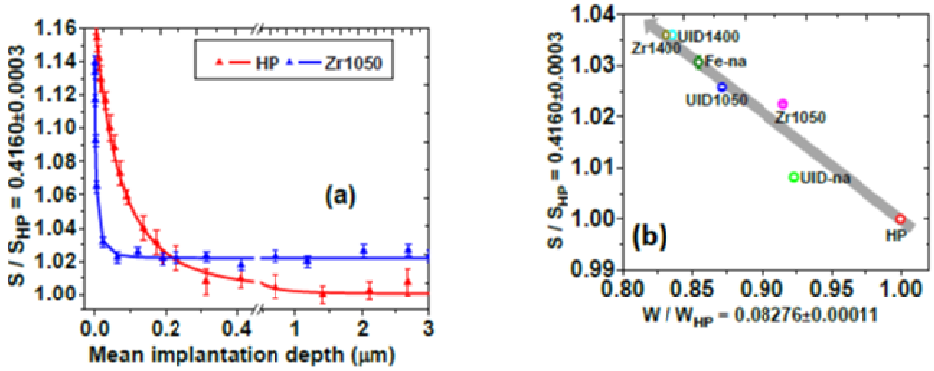

FIG. 6, (a) Depth profile of *S*-parameter for HP and O_2 annealed Zr doped samples, and (b) *S* vs. *W* plot, for HP, O_2 annealed Zr doped, Fe-na, and the UID samples with both as grown and O_2 annealed conditions.

We next estimated c_d from diffusion length *L*, which favorably showed less sensitivity to orientation and a larger dynamic range. The *S* parameter for the HP sample shows a gradual trend from annihilations at the surface (typically high *S* values) to a constant value of *S* deep in the sample (>1 μm), with a value of S_b = 0.4160±0.0003 that is the lowest among all samples. The *L* value for the HP sample is the longest measured at 92±8 nm, close to what is expected in

high quality defect-free material, and is chosen as L_b in this study. The O_2 annealed sample shows a much more rapid initial decrease with implantation depth, and the *S* levels off much closer to the surface to a constant value of *S*. The *S* value for all the annealed samples is 2.25% to >3% above that for the HP sample, corresponding to short diffusion lengths between *L*~6 nm to 10 nm.

It should be noted that a shorter diffusion length may also be interpreted as presence of a positive potential at the surface that would repel positrons towards the bulk. Such a possibility is ruled out here. Firstly, the data shown in Fig. 6 indicate a significant increase in *S* parameter after annealing, suggesting the presence of vacancies or their complexes or clusters that trap positrons. As the concentration of these defects increases, the diffusion length must decrease. The directly observed increase in *S* and the sharper transition with depth from the surface *S* value to the bulk *S* value, i.e., shorter diffusion length, both match our interpretation. Secondly, Lovejoy et al. discussed electric fields due to band bending in Ga_2O_3 and reported a potential caused by surface defects of only 0.5 V, positive at the surface, and extending to ~ 7 nm into the bulk [41]. Modeling PAS data with these parameters and a long diffusion length leads to poor fitting to the observed data. The shallow range of the electric field is incompatible with a long diffusion length and the observed data.

Defect concentrations estimated using equation 3, using the diffusion length, fall in the range (3-8) $\times 10^{18}$ cm^{-3} for all the annealed sample with approximately 20% uncertainty. The data trend for the Fe-doped sample has the second longest diffusion length, *L*=27±2 nm, which correspond to c_d ~3.8×10^{17} cm^{-3}. However, the *S* value for this sample is the second highest. The discrepancy in the trend between *L* and *S*, as well as the small deviation from straight line for some of the samples on the *S*-*W* plot, are likely the effect of orientation-dependent anisotropy.

Regarding the origin of the open volume defect, we note from Fig. 6 (b) that the bulk *S* and *W* values for all the samples fall close to a straight line, suggesting one type of open volume defect in all the samples. Under O_2-rich annealing conditions, the formation of gallium vacancies (or oxygen interstitials) is energetically favored, and an increased density of vacancies has been observed by PAS on oxygen-annealed Si and Sn doped samples [42]. In addition, theoretical calculations indicate that oxygen vacancies are too small to trap positrons [43]. Therefore, the small observed change in the PAS signal is due to either a few large open volume defects such as $V_{Ga} - V_O$ complexes or due to high concentrations of smaller open volume defects. The latter scenario is consistent with the model of resistivity based on the observed traps, estimated trap concentration, and short positron diffusion length.

The PAS results also supports reported observations on Ga_2O_3. The range from defect-free S_b to saturation value S_d is rather small, with 2-3% variation compared to a more common 4-6% range in other materials such as GaN and ZnO, an effect that is attributed to atypical relaxation of atoms near a gallium vacancy [34]. A near neighboring Ga atom moves into the center of the vacancy resulting in two smaller open volumes or split vacancies ($2V_{Ga}$-Ga_i) also designated as V^i_{Ga}; these structures have been predicted by density functional theory and observed by scanning transmission electron microscopy [44].

Hydrogen plays a major role in Ga_2O_3, and can occupy the open volume in the split Ga vacancy since it has been well documented to form OH bonds and cannot exist in unrelaxed vacancies [17]. This would lower the positron Doppler signal *S*. Here, care was taken to avoid exposure to hydrogen during annealing and none was observed to be present in Fourier-transform infrared (FTIR) spectroscopy in as grown unintentionally doped (UID) material.

Furthermore, introduction of hydrogen would be inconsistent with increasing resistivity, as it can passivate these acceptor states.

This indicates that the open volume defect seen here is not likely to involve neutral oxygen vacancy (V_O), dopants, hydrogen, or their complexes with V_{Ga}. The results strongly point towards split gallium vacancies as the defect identified with TEES at a depth of 0.73 eV (E2*) below the conduction band that is responsible for the observed strong compensation of the shallow Zr donors after O_2 annealing.

IV. CONCLUSION

In summary, a defect level at ≈0.73 eV (E2*) with concentration ≈10^{18} cm^{-3} is found to be responsible for more than 10 order of magnitude increase in resistivity in O_2 annealed samples doped with shallow donors (Zr). Observations of a lower than typical range of variation in positron *S*-parameter and the high concentration of open volume defects estimated from the measured positron diffusion length supports similar PAS observations and is consistent with a model of compensation based on split gallium vacancies. Careful positron measurements, as shown here, can quantify the concentration, in spite of anisotropy of the *S* value, which depends on sample orientation with respect to incident positrons and collected annihilations. The positron diffusion length can be determined independently of the sample orientation and can provide more reliable information on open volume vacancy-like defect concentrations for Ga_2O_3 and other materials with similar challenges.

ACKNOWLEDGEMENTS

This material is based upon work supported by the Air Force Office of Scientific Research under award number FA9550-18-1-0507 (Program Manager: Dr. Ali Sayir). Any opinions, finding, and conclusions or recommendations expressed in this material are those of the authors and do not necessarily reflect the views of the United States Air Force. The authors thank Arkka Bhattacharya and Sriram Krishnamurty of University of Utah for making electrical contact on some of the samples. We would also like to thank Prof. Michael Scarpulla of University of Utah and John Blevins of Air Force Research Laboratory for providing Fe doped samples and powder for producing the HP crystal.

Data availability: The data that support the findings of this study are available from the corresponding author upon reasonable request.

REFERENCES

[1] A. E. Romanov, S. I. Stepanov, V. I. Nikolaev, and V. E. Bougrov, GALLIUM OXIDE: PROPERTIES AND APPLICA A REVIEW, 2016.

[2] P. Jaiswal, U. Ul Muazzam, A. S. Pratiyush, N. Mohan, S. Raghavan, R. Muralidharan, S. A. Shivashankar, and D. N. Nath, *Microwave Irradiation-Assisted Deposition of Ga2O3 on III-Nitrides for Deep-UV Opto-Electronics*, Appl. Phys. Lett. **112**, 021105 (2018).

[3] M. Higashiwaki, A. Kuramata, H. Murakami, and Y. Kumagai, *State-of-the-Art Technologies of Gallium Oxide Power Devices*, Journal of Physics D: Applied Physics.

[4] Y. J. Wu, C. H. Hsieh, P. H. Chen, J. Y. Li, L. J. Chou, and L. J. Chen, *Plasmon Resonance Spectroscopy of Gold-in-Gallium Oxide Peapod and Core/Shell Nanowires*, ACS Nano **4**, 1393 (2010).

[5] M. Higashiwaki, K. Sasaki, A. Kuramata, T. Masui, and S. Yamakoshi, *Development of Gallium Oxide Power Devices*, Phys. Status Solidi Appl. Mater. Sci. **211**, 21 (2014).

[6] Z. Hu, K. Nomoto, W. Li, N. Tanen, K. Sasaki, A. Kuramata, T. Nakamura, D. Jena, and H. G. Xing, *Enhancement-Mode Ga2O3 Vertical Transistors with Breakdown Voltage >1 KV*, IEEE Electron Device Lett. **39**, 869 (2018).

[7] J. Xu, W. Zheng, and F. Huang, *Gallium Oxide Solar-Blind Ultraviolet Photodetectors: A Review*, Journal of Materials Chemistry C.

[8] D. Agarwal, C. O. Aspetti, M. Cargnello, M. L. Ren, J. Yoo, C. B. Murray, and R. Agarwal, *Engineering Localized Surface Plasmon Interactions in Gold by Silicon Nanowire for Enhanced Heating and Photocatalysis*, Nano Lett. **17**, 1839 (2017).

[9] M. J. Tadjer, J. L. Lyons, N. Nepal, J. A. Freitas, A. D. Koehler, and G. M. Foster, *Editors' Choice—Review—Theory and Characterization of Doping and Defects in β-Ga 2 O 3* , ECS J. Solid State Sci. Technol. **8**, Q3187 (2019).

[10] A. T. Neal, S. Mou, S. Rafique, H. Zhao, E. Ahmadi, J. S. Speck, K. T. Stevens, J. D. Blevins, D. B. Thomson, N. Moser, K. D. Chabak, and G. H. Jessen, *Donors and Deep Acceptors in β-Ga2O3*, Appl. Phys. Lett. **113**, 062101 (2018).

[11] M. Saleh, A. Bhattacharyya, J. B. Varley, S. Swain, J. Jesenovec, S. Krishnamoorthy, and K. Lynn, *Electrical and Optical Properties of Zr Doped β-Ga2O3 Single Crystals*, Appl. Phys. Express **12**, 085502 (2019).

[12] M. Saleh, J. B. Varley, J. Jesenovec, A. Bhattacharyya, S. Krishnamoorthy, S. Swain, and K. Lynn, *Degenerate Doping in β-Ga2O3 Single Crystals through Hf-Doping*, Semicond. Sci. Technol. **35**, 04LT01 (2020).

[13] P. Deák, Q. Duy Ho, F. Seemann, B. Aradi, M. Lorke, and T. Frauenheim, *Choosing the Correct Hybrid for Defect Calculations: A Case Study on Intrinsic Carrier Trapping in β-G A2 O3*, Phys. Rev. B **95**, 075208 (2017).

[14] J. B. Varley, H. Peelaers, A. Janotti, and C. G. Van De Walle, *Hydrogenated Cation Vacancies in Semiconducting Oxides*, J. Phys. Condens. Matter **23**, 334212 (2011).

[15] C. Zimmermann, E. Frdestrom Verhoeven, Y. Kalmann Frodason, P. M. Weiser, J. B. Varley, and L. Vines, *Formation and Control of the E*2 Center in Implanted β-Ga2O3 by Reverse-Bias and Zero-Bias Annealing*, J. Phys. D. Appl. Phys. **53**, 9 (2020).

[16] B. E. Kananen, L. E. Halliburton, K. T. Stevens, G. K. Foundos, and N. C. Giles, *Gallium Vacancies in β-Ga2O3 Crystals*, Appl. Phys. Lett. **110**, 202104 (2017).

[17] P. Weiser, M. Stavola, W. B. Fowler, Y. Qin, and S. Pearton, *Structure and Vibrational Properties of the Dominant O-H Center in β-Ga2O3*, Appl. Phys. Lett. **112**, 232104 (2018).

[18] M. D. McCluskey, *Point Defects in Ga2O3*, J. Appl. Phys. **127**, 101101 (2020).

[19] E. Korhonen, F. Tuomisto, D. Gogova, G. Wagner, M. Baldini, Z. Galazka, R. Schewski, and M. Albrecht, *Electrical Compensation by Ga Vacancies in Ga2O3 Thin Films*, Appl. Phys. Lett. **106**, 242103 (2015).

[20] P. Saadatkia, S. Agarwal, A. Hernandez, E. Reed, I. D. Brackenbury, C. L. Codding, M. O. Liedke, M. Butterling, A. Wagner, and F. A. Selim, *Point and Extended Defects in Heteroepitaxial β- G A2 O3 Films*, Phys. Rev. Mater. **4**, 104602 (2020).

[21] A. Y. Polyakov, N. B. Smirnov, I. V. Shchemerov, D. Gogova, S. A. Tarelkin, and S. J. Pearton, *Compensation and Persistent Photocapacitance in Homoepitaxial Sn-Doped β-Ga2O3*, J. Appl. Phys. **123**, 115702 (2018).

[22] M. M. Islam, N. Adhikari, A. Hernandez, A. Janover, S. Novak, S. Agarwal, C. L. Codding, M. Snure, M. Huang, and F. A. Selim, *Direct Measurement of the Density and Energy Level of Compensating Acceptors and Their Impact on the Conductivity of N-Type Ga2O3 Films*, J. Appl. Phys. **127**, 145701 (2020).

[23] A. Y. Polyakov, N. B. Smirnov, I. V. Shchemerov, E. B. Yakimov, S. J. Pearton, C. Fares, J. Yang, F. Ren, J. Kim, P. B. Lagov, V. S. Stolbunov, and A. Kochkova, *Defects Responsible for Charge Carrier Removal and Correlation with Deep Level Introduction in Irradiated β-Ga2O3*, Appl. Phys. Lett. **113**, 092102 (2018).

[24] K. Irmscher, Z. Galazka, M. Pietsch, R. Uecker, and R. Fornari, *Electrical Properties of β-Ga2O3 Single Crystals Grown by the Czochralski Method*, J. Appl. Phys. **110**, 063720 (2011).

[25] R. Sun, Y. K. Ooi, A. Bhattacharyya, M. Saleh, S. Krishnamoorthy, K. G. Lynn, and M. A. Scarpulla, *Defect States and Their Electric Field-Enhanced Electron Thermal Emission in Heavily Zr-Doped β -Ga2O3crystals*, Appl. Phys. Lett. **117**, 212104 (2020).

[26] P. J. Schultz and K. G. Lynn, *Interaction of Positron Beams with Surfaces, Thin Films, and Interfaces*, Rev. Mod. Phys. **60**, 701 (1988).

[27] F. Tuomisto and I. Makkonen, *Defect Identification in Semiconductors with Positron Annihilation: Experiment and Theory*, Rev. Mod. Phys. **85**, 1583 (2013).

[28] B. Šantić and U. V. Desnica, *Thermoelectric Effect Spectroscopy of Deep Levels - Application to Semi-Insulating GaAs*, Appl. Phys. Lett. **56**, 2636 (1990).

[29] U. V. Desnica, M. Pavlović, Z. Q. Fang, and D. C. Look, *Thermoelectric Effect Spectroscopy of Deep Levels in Semi-Insulating GaN*, J. Appl. Phys. **92**, 4126 (2002).

[30] C. Szeles, Y. Shan, K. Lynn, A. Moodenbaugh, and E. Eissler, *Trapping Properties of Cadmium Vacancies ITe*, Phys. Rev. B - Condens. Matter Mater. Phys. **55**, 6945 (1997).

[31] T. Ablekim, S. K. Swain, W. J. Yin, K. Zaunbrecher, J. Burst, T. M. Barnes, D. Kuciauskas, S. H. Wei, and K. G. Lynn, *Self-Compensation in Arsenic Doping of CdTe*, Sci. Rep. **7**, 1 (2017).

[32] K. H. Nicholas and J. Woods, *The Evaluation of Electron Trapping Parameters from Conductivity Glow Curves in Cadmium Sulphide*, Br. J. Appl. Phys. **15**, 783 (1964).

[33] E. Korhonen, F. Tuomisto, O. Bierwagen, J. S. Speck, and Z. Galazka, *Compensating Vacancy Defects in Sn- and Mg-Doped In2 O3*, Phys. Rev. B - Condens. Matter Mater. Phys. **90**, 245307 (2014).

[34] A. Karjalainen, V. Prozheeva, K. Simula, I. Makkonen, V. Callewaert, J. B. Varley, and F. Tuomisto, *Split Ga Vacancies and the Unusually Strong Anisotropy of Positron Annihilation Spectra in β-Ga2 O3*, Phys. Rev. B **102**, 195207 (2020).

[35] J. B. Varley, H. Peelaers, A. Janotti, and C. G. Van De Walle, *Hydrogenated Cation Vacancies in Semiconducting Oxides*, J. Phys. Condens. Matter (2011).

[36] A. Y. Polyakov, N. B. Smirnov, I. V. Shchemerov, S. J. Pearton, F. Ren, A. V. Chernykh,

and A. I. Kochkova, *Electrical Properties of Bulk Semi-Insulating β-Ga2O3 (Fe)*, Appl. Phys. Lett. **113**, 142102 (2018).

[37] M. E. Ingebrigtsen, J. B. Varley, A. Y. Kuznetsov, B. G. Svensson, G. Alfieri, A. Mihaila, U. Badstübner, and L. Vines, *Iron and Intrinsic Deep Level States in Ga2O3*, Appl. Phys. Lett. **112**, 042104 (2018).

[38] Z. Zhang, E. Farzana, A. R. Arehart, and S. A. Ringel, *Deep Level Defects throughout the Bandgap of (010) β-Ga2O3 Detected by Optically and Thermally Stimulated Defect Spectroscopy*, Appl. Phys. Lett. **108**, 052105 (2016).

[39] B. Wang, D. Look, and K. Leedy, *Deep Level Defects in β-Ga2O3 Pulsed Laser Deposited Thin Films and Czochralski-Grown Bulk Single Crystals by Thermally Stimulated Techniques*, J. Appl. Phys. **125**, 105103 (2019).

[40] A. van Veen, H. Schut, M. Clement, J. M. M. de Nijs, A. Kruseman, and M. R. IJpma, *VEPFIT Applied to Depth Profiling Problems*, Appl. Surf. Sci. **85**, 216 (1995).

[41] T. C. Lovejoy, R. Chen, X. Zheng, E. G. Villora, K. Shimamura, H. Yoshikawa, Y. Yamashita, S. Ueda, K. Kobayashi, S. T. Dunham, F. S. Ohuchi, and M. A. Olmstead, *Band Bending and Surface Defects in β-Ga 2O 3*, Appl. Phys. Lett. **100**, 181602 (2012).

[42] M. J. Tadjer, J. A. Freitas, J. C. Culbertson, M. H. Weber, E. R. Glaser, A. L. Mock, N. A. Mahadik, K. Schmieder, E. Jackson, J. C. Gallagher, B. N. Feigelson, and A. Kuramata, *Structural and Electronic Properties of Si- And Sn-Doped (-201) β-Ga2O3 Annealed in Nitrogen and Oxygen Atmospheres*, J. Phys. D. Appl. Phys. **53**, 504002 (2020).

[43] I. Makkonen, E. Korhonen, V. Prozheeva, and F. Tuomisto, *Identification of Vacancy Defect Complexes in Transparent Semiconducting Oxides ZnO, In2O3 and SnO2*, J. Phys. Condens. Matter **28**, 224002 (2016).

[44] J. M. Johnson, Z. Chen, J. B. Varley, C. M. Jackson, E. Farzana, Z. Zhang, A. R. Arehart, H. L. Huang, A. Genc, S. A. Ringel, C. G. Van De Walle, D. A. Muller, and J. Hwang, *Unusual Formation of Point-Defect Complexes in the Ultrawide-Band-Gap Semiconductor β-Ga2 O3*, Phys. Rev. X **9**, 041027 (2019).